NASA TN D-1073

TECHNICAL NOTE

D-1073

STUDY OF A SATELLITE ATTITUDE CONTROL SYSTEM

USING INTEGRATING GYROS AS TORQUE SOURCES

By John S. White and Q. Marion Hansen

Ames Research Center
Moffett Field, Calif.

NATIONAL AERONAUTICS AND SPACE ADMINISTRATION

WASHINGTON

September 1961

NATIONAL AERONAUTICS AND SPACE ADMINISTRATION

TECHNICAL NOTE D-1073

STUDY OF A SATELLITE ATTITUDE CONTROL SYSTEM USING INTEGRATING GYROS AS TORQUE SOURCES

By John S. White and Q. Marion Hansen

SUMMARY

This report considers the use of single-degree-of-freedom integrating gyros as torque sources for precise control of satellite attitude. Some general design criteria are derived and applied to the specific example of the Orbiting Astronomical Observatory. The results of the analytical design are compared with the results of an analog computer study and also with experimental results from a low-friction platform. The steady-state and transient behavior of the system, as determined by the analysis, by the analog study, and by the experimental platform agreed quite well.

The results of this study show that systems using integrating gyros for precise satellite attitude control can be designed to have a reasonably rapid and well-damped transient response, as well as very small steady-state errors. Furthermore, it is shown that the gyros act as rate sensors, as well as torque sources, so that no rate stabilization networks are required, and when no error sensor is available, the vehicle is still rate stabilized. Hence, it is shown that a major advantage of a gyro control system is that when the target is occulted, an alternate reference is not required.

INTRODUCTION

For most satellites some form of attitude control is required, and in many cases the control must be fairly precise. This report will discuss the use of integrating gyros as torque sources to obtain precise satellite attitude control. Similar discussions of systems using motor-driven inertia wheels and the earth's magnetic field are given in references 1 and 2.

The requirements placed on satellite attitude control systems vary from one satellite to another; however, it can be stated generally that a reference, or tracking line, in the satellite is required to be maintained in alinement with a specified external reference, or line of sight, to a specified accuracy. This must be accomplished in the presence of disturbing torques and apparent motion of the external reference.

Motion of the external reference may be oscillatory at the orbital period, as a result of parallax or velocity aberration, or it may be nearly constant, as in the case of an earth-pointing satellite. Disturbing torques acting on an earth satellite might come from the earth's gravity gradient, the sun's radiation pressure, the earth's atmospheric density, and the earth's magnetic field.

An earth satellite which is currently being studied by NASA and which will serve as an example for gyro system control in this report is the Orbiting Astronomical Observatory. The OAO will contain one or more telescopes, to be used primarily for obtaining photometric and spectrographic data from ultraviolet star radiation above the earth's atmosphere. The specific precise control requirements of the OAO, which will be used as an example in this report, demand that the pointing error of the telescope (rigidly attached to the vehicle) be reduced from 1 minute of arc to less than 0.1 second of arc within 2 or 3 minutes of time, and the error maintained at less than 0.1 second of arc for one orbital period of approximately 100 minutes. Furthermore, roll motion about the line of sight must be maintained at less than 1 second of arc per second. For solar sighting, the line-of-sight velocity, due to apparent motion of the external reference, will have a maximum of 0.01 second of arc per second, predominantly from parallax effects. For stellar sighting, the line-of-sight velocity will have a maximum of 0.005 second of arc per second, predominantly from velocity aberration effects. Both of these line-of-sight velocity effects are calculated in reference 1. The disturbance torques were assumed to be on the order of 100 dyne centimeters. A description of the torque inputs leading to this estimate may be found in reference 3.

A 4 4 3

In this report a physical explanation of the use of a gyro as a torque source for a satellite is followed by a derivation and discussion of the equations for a single-degree-of-freedom gyro. The over-all system equations are then developed, both open loop and closed loop, and the system errors are discussed. The equations derived are then normalized and simplified to allow easy visualization of the system response characteristics. A sample system based on the example of the OAO is designed, and the results of a three-axis analog study are discussed. Finally, a comparison is made between theoretical, analog, and experimental results for a single-axis system.

NOTATION

A_f	gyro float angle, radians
C	gyro damping constant, dyne cm sec
H	gyro angular momentum, dyne cm sec

H_s	stored angular momentum, dyne cm sec
I_b	moment of inertia of vehicle, gm cm^2
I_f	moment of inertia of gyro float, gm cm^2
K_{TG}	over-all gain from sensor to torque generator, (dyne cm)/radian
s	Laplace operator, sec^{-1}
t	time, sec
t_c	duration of time during which vehicle is to be controlled, sec
t_{lim}	time during which error signal is limited, sec
t_{set}	settling time, sec
T_c	control torque or gyro output torque, dyne cm
T_d	disturbance torque exerted on body by external sources, dyne cm
T_{TG}	torque exerted on gyro float by torque generator, dyne cm
T_{UG}	uncertainty in the torque exerted on gyro float, dyne cm
x,y,z	axes of a right-hand orthogonal coordinate system
ζ	normalized damping ratio
τ	time constant, sec
τ_n	natural period, $\frac{2\pi}{\omega_n}$, sec
φ_b	angle between tracking line and reference, radians
φ_e	error in pointing, radians
$\varphi_{e_{lim}}$	effective limit level of error detector, radians
φ_{LS}	angle between line of sight and reference, radians
ω_b	angular velocity of vehicle, radians/sec
ω_f	angular velocity of gyro float, radians/sec
ω_{LS}	angular velocity of line of sight, radians/sec

ω_n natural frequency of over-all control system, radians/sec

$(\bar{\ })$ vector quantity

Subscripts

o initial value

ol open loop

ss steady state

max maximum allowable value of quantity

GENERAL SYSTEM DISCUSSION

A simplified block diagram of a single-axis control system that uses an integrating gyro as a torque source is shown in sketch (a):

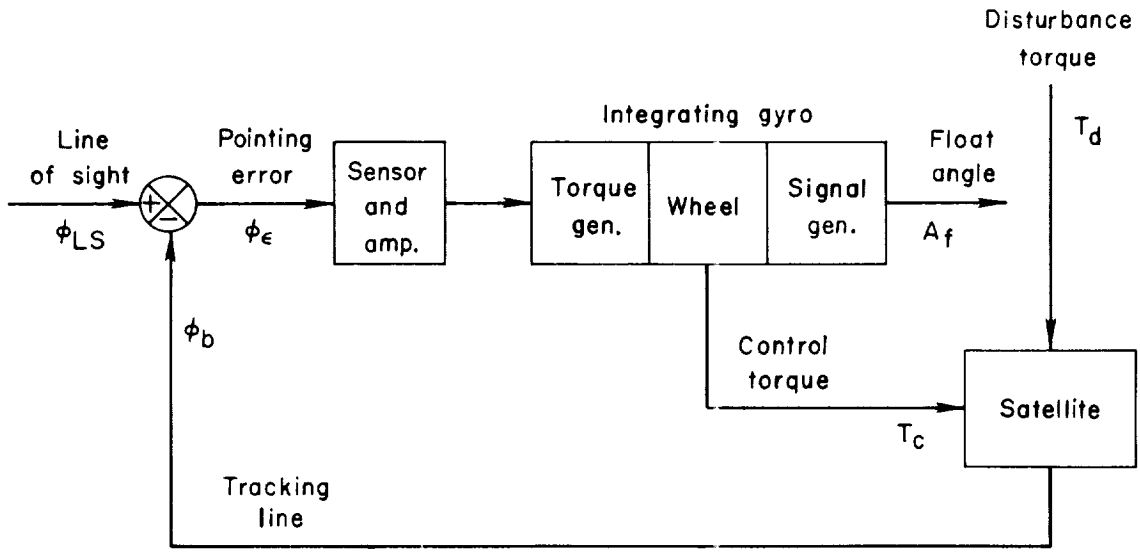

Sketch (a)

The basic command loop consists of a sensor to detect pointing error, φ_e, an integrating gyro, which produces a control torque, T_c, acting on the satellite, and finally the satellite itself, which includes a rigidly attached telescope.

The gyros are also rigidly attached to the satellite, with both the gyro float axis and the spin reference axis perpendicular to the axis about which it is desired to exert a torque on the satellite. Figure 1 is a pictorial view of one of the gyros, including the angular momentum vector, $\overline{H}$, along the spin axis, the float angular velocity vector, $\overline{\omega}_f$, along the float axis, and the resultant control torque vector, $\overline{T}_c$, along the gyro sensitive axis. The gyro serves both as a source of control torque and as a rate stabilizing device. This can be seen as follows: If a torque is exerted about the gyro float axis, either by the torque generator or by an angular velocity of the vehicle about the gyro sensitive axis, the float will move about the gyro float axis at a rate, ω_f, (assuming a gyro with fluid damping) proportional to the torque. The rate of rotation of the gyro float produces a torque, $\overline{T}_c = \overline{\omega}_f \times \overline{H}$, about the sensitive axis. When T_c is caused by angular velocity of the satellite, ω_b, then T_c will be in a direction to reduce the satellite angular velocity resulting in rate stabilization. When T_c is caused by the torque generator the gyro will again exert a torque on the satellite about the sensitive axis.

A
4
4
3

The amount of control torque available about the gyro sensitive axis will depend on the velocity of the gyro float about the float axis, and this in turn, in the steady state, is inversely proportional to the damping of the gyro; that is, for a given input torque to the float, if the damping is reduced, the steady angular velocity of the float, and hence the output torque, will be increased. The system response, however, will become more oscillatory; thus, the selection of damping will depend on the production of a sufficient amount of control torque without the response becoming too oscillatory.

It should be noted that if it is desired to obtain a constant vehicle velocity about the gyro sensitive axis, the gyro float velocity must be zero to maintain constant angular momentum (assuming zero disturbance torque acting on the satellite). The torque generator must thus put out a steady-state torque, T_{TG}, sufficient to cancel the gyroscopic torque, $\overline{\omega}_b \times \overline{H}$, acting on the float. This torque-generator torque will be independent of the damping and will react on the vehicle about one of the other control axes, producing cross coupling. One possible means for eliminating this cross coupling is to use two counterrotating gyros for each axis. Then the torque from the torque generator of one gyro will cancel that from the other gyro, and there will be no net cross-coupling torque on the satellite. However, for the example, where the gyros are used to maintain the vehicle essentially inertially fixed in space, this cross coupling is found to be negligible.

There are two disturbances to be considered, as previously mentioned: an angular velocity of the line of sight, and an external disturbance torque acting on the satellite. Consider first the effect of a constant angular velocity of the line of sight. In the steady-state condition, the gyro float angle will be constant, as previously noted, and the net torque acting on the gyro float must be zero. The torque created by the

angular velocity of the vehicle about the gyro sensitive axis (to follow the line of sight) must be exactly canceled by the torque from the torque generator. This latter torque, for the system shown in sketch (a), is proportional to the tracking error.

Next, consider only the effect of external torque on the system. To counter this torque, the gyro must have a constant velocity about its float axis, which, since the gyro is damped, requires a constant torque from the torque generator. Since the satellite is not rotating there will be no torque on the float from gyroscopic precession. Again, the torque from the torque generator is proportional to the tracking error.

Thus, to correct for either type of disturbance, there must be a steady-state pointing error, and to keep this pointing error small the sensor and amplifier gains must be quite large.

DERIVATION OF SYSTEM EQUATIONS

Gyro Transfer Function

The block diagram of an integrating gyro is shown in sketch (b):

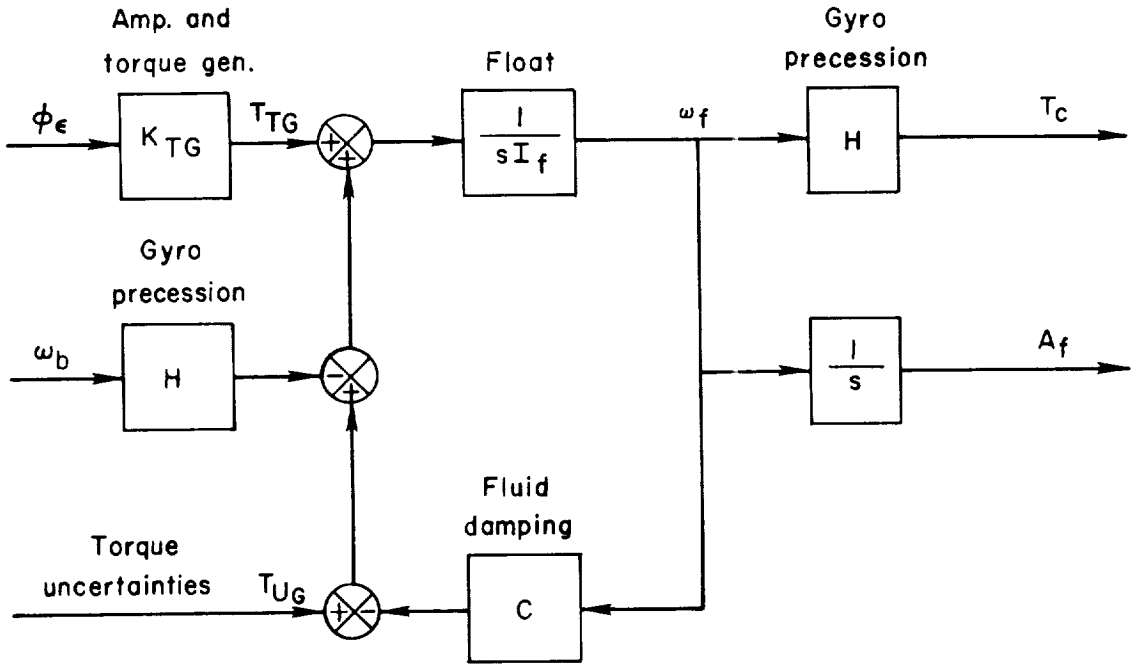

Sketch (b)

The three summing points shown represent the torque summing action of the gyro float, with the net resultant torque being available to accelerate the float, and thus produce an angular velocity of the float, ω_f. The torque inputs to the gyro about the float axis are from the torque generator, T_{TG}; an uncertainty, T_{UG}, resulting from gravity unbalance, spring torques, etc.; the gyro precession, $-\omega_b H$, which is perpendicular to $\bar{\omega}_b$ and $\bar{H}$; and fluid damping, $-\omega_f C$. Float velocity, ω_f, resulting from the summation of these torques produces an output control torque, $T_c = \omega_f H$, about the sensitive axis.

The over-all gyro equations obtained from sketch (b) are

$$A_f = \frac{\frac{1}{sC}\left(T_{TG} + T_{UG} - H\omega_b\right)}{1 + s(I_f/C)} \tag{1}$$

$$T_c = H\omega_f = \frac{H}{C}\left[\frac{T_{TG} + T_{UG} - H\omega_b}{1 + s(I_f/C)}\right] \tag{2}$$

Equation (2) shows that the gyro can have a torque multiplying effect (provided $H/C > 1$), so that the control torque exerted on the body can be many times larger than that exerted by the torque generator on the gyro float.

The complete block diagram for single-axis control is shown in sketch (c).

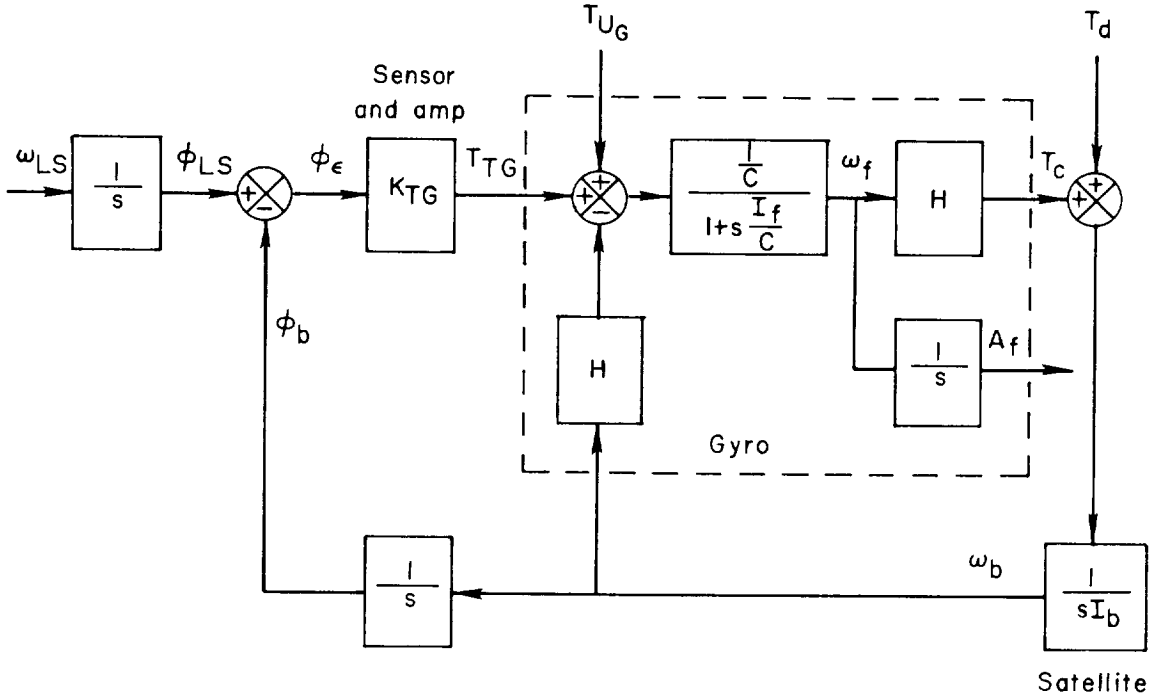

Sketch (c)

The gyro representation is simplified from that of sketch (b) by use of the transfer functions of equations (1) and (2). Included are the external disturbance torque, T_d, acting on the satellite, and the uncertainty torque, T_{U_G}, acting on the gyro float. The gyro float angle, A_f, is not used in this application, except as a measure of the amount of momentum stored.

It should be noted that the torque from the torque generator, T_{TG}, the uncertainties, T_{U_G}, and the damping, $C\omega_f$, all act on the float and react on the case, so that these reactions appear as disturbing torques about one of the other satellite axes. However, in the steady state their values will be much smaller than the control torque, T_c, and so will not seriously affect the response of the system.

A
4
4
3

Open-Loop Transfer Functions

The open-loop transfer functions applicable to sketch (c), assuming the loop is broken at point A, are:

For angular velocity of the vehicle;

$$\omega_{b_{o1}} = \frac{T_d \frac{C}{H^2}\left(s\frac{I_f}{C} + 1\right) + (T_{U_G} + T_{TG})\frac{1}{H}}{s^2\frac{I_b I_f}{H^2} + s\frac{I_b C}{H^2} + 1} \tag{3}$$

For gyro float angle;

$$A_{f_{o1}} = \frac{(T_{U_G} + T_{TG})\frac{I_b}{H^2} - \frac{T_d}{H}\frac{1}{s}}{s^2\frac{I_b I_f}{H^2} + s\frac{I_b C}{H^2} + 1} \tag{4}$$

Closed-Loop Transfer Functions

If the loop is now closed, the relation

$$T_{TG} = \frac{K_{TG}}{s}(\omega_{LS} - \omega_b) \tag{5}$$

can be used to obtain the closed-loop transfer functions. From equations (3) and (5), the angular velocity equation is found

$$\omega_b = \frac{\omega_{LS} + \frac{T_d}{s}\frac{C}{HK_{TG}}\left(s\frac{I_f}{C} + 1\right) + \frac{T_{U_G}}{s}\frac{1}{K_{TG}}}{s^3\frac{I_bI_f}{HK_{TG}} + s^2\frac{I_bC}{HK_{TG}} + s\frac{H}{K_{TG}} + 1} \tag{6}$$

Since the chief concern is the magnitude of the error angle, φ_e, the closed-loop error equation is desired. Using the relationship

$$\omega_b = \omega_{LS} - s\varphi_e \tag{7}$$

A 4 4 3

and solving for φ_e gives the desired equation:

$$\varphi_e = \frac{\omega_{LS}\frac{H}{K_{TG}}\left(s^2\frac{I_bI_f}{H^2} + s\frac{I_bC}{H^2} + 1\right) - T_d\frac{C}{HK_{TG}}\left(s\frac{I_f}{C} + 1\right) - T_{U_G}\frac{1}{K_{TG}}}{s^3\frac{I_bI_f}{HK_{TG}} + s^2\frac{I_bC}{HK_{TG}} + s\frac{H}{K_{TG}} + 1} \tag{8}$$

The associated float angle, A_f, found by substituting

$$T_{TG} = \left(\omega_{LS} - \frac{sA_fH + T_d}{sI_b}\right)\frac{K_{TG}}{s} \tag{9}$$

into equation (4), is

$$A_f = \frac{\omega_{LS}\frac{I_b}{H} - \frac{T_d}{s}\left(s\frac{H}{K_{TG}} + 1\right)\frac{1}{H} + T_{U_G}\frac{sI_b}{HK_{TG}}}{s^3\frac{I_bI_f}{HK_{TG}} + s^2\frac{I_bC}{HK_{TG}} + s\frac{H}{K_{TG}} + 1} \tag{10}$$

Steady-State Considerations

Consider first the condition when the object star is occulted by the earth; that is, $K_{TG} = 0$. Applying the final-value theorem for step inputs of T_d, T_{U_G}, and T_{TG} to equation (3) gives

$$\omega_{b_{occ_{ss}}} = T_d\frac{C}{H^2} + T_{U_G}\frac{1}{H} + T_{TG}\frac{1}{H} \tag{11}$$

It is interesting to note that the resultant steady-state satellite angular velocity is independent of the satellite moment of inertia. This can be seen physically by realizing that for $T_{TG} = 0$ the control torque, T_c, generated by the gyro depends mostly on vehicle angular velocity, and when this torque equals the disturbance torque, T_d, there will be no further change in the vehicle velocity. Furthermore, equation (11) points out a great advantage of the gyro system over other types of control systems, namely rate stabilization. Thus, without an error detector, the vehicle will assume an angular velocity which varies linearly with and is approximately proportional to the disturbing torque. This can be compared to the angular velocity of a vehicle, still with no error detector, but also with no gyro aboard. In this latter case the external torque produces a constant acceleration, and so the angular velocity will increase at a steady rate, that is

A 4 4 3

$$\omega'_{b_{o1_{ss}}} \approx \frac{T_d}{I_b} t \tag{12}$$

If equations (11) and (12) are integrated, the effectiveness of this rate stabilization can be determined. After a reasonable period of occultation, it is found that for many pratical applications, the error angle with the gyro control system is much smaller than that for the uncontrolled case. In the OAO example, the error for the uncontrolled case might be much greater than the range of the error detector, while for the gyro-controlled case, the error would remain within the range of the error detector so that the gyros would eliminate the need for switching to a coarse control system following occultation.

For the occulted condition the steady-state float angle may also be found if the inverse transform of equation (4) is simplified for large values of t.

$$A_{f_{o1_{ss}}} \approx - \frac{T_d}{H} t \tag{13}$$

This equation shows that the float angle will increase constantly with time, and thus that the gyro momentum vector rotates to cancel the effect of the external torque.

For the complete system, with a signal available from the error detector, the steady-state equations obtained from equations (8) and (10) are:

$$\varphi_{e_{ss}} = \omega_{LS} \frac{H}{K_{TG}} - T_d \frac{C}{HK_{TG}} - \frac{T_{U_G}}{K_{TG}} \tag{14}$$

$$A_{f_{ss}} \approx \omega_{LS} \frac{I_b}{H} - \frac{T_d}{H} t \tag{15}$$

The sighting error, $\varphi_{e_{ss}}$, reaches a steady-state value which can be made small with proper design. The portion of the float angle, $A_{f_{ss}}$, resulting from ω_{LS} is a relatively small constant, but that from the disturbance torque increases directly with time. This is to be expected, since it shows that the gyro is storing the momentum resulting from the external torques.

NORMALIZED DESIGN

A 4 4 3

In the actual design of a control system, the first considerations are the amount of disturbance torque expected and the length of the time, t_c, over which the control system must counter this torque. These two factors determine the amount of momentum which the control system must be able to store.

Since torque is the time derivative of momentum, the stored momentum, H_s, must equal $\int T_d\, dt$. If a constant disturbance torque is applied for the duration of the control time, the maximum stored momentum becomes $H_{s_{max}} = T_d t_c$. In turn, the stored momentum will be the product of gyro wheel momentum, H, and the sine of the float angle, A_f. Since the float angle must be limited to relatively small angles to avoid excessive cross coupling, sine $A_f \cong A_f$. Hence,

$$H = \frac{H_{s_{max}}}{A_{f_{max}}} = \frac{T_d t_c}{A_{f_{max}}} \tag{16}$$

which will allow the determination of H.

Once a value for H is selected, it seems reasonable to normalize all other variables with respect to this value. When this is done, the equations previously derived take the following forms: For the open loop, from equations (3) and (4),

$$\omega_{b_{ol}} = \frac{\frac{T_d}{H}\frac{C}{H}\left(s\frac{I_f}{H}\frac{H}{C} + 1\right) + \frac{T_{U_G}}{H} + \frac{T_{TG}}{H}}{s^2\frac{I_b}{H}\frac{I_f}{H} + s\frac{I_b}{H}\frac{C}{H} + 1} \tag{17}$$

$$A_{f_{ol}} = \frac{\left(\frac{T_{U_G}}{H} + \frac{T_{TG}}{H}\right)\frac{I_b}{H} - \frac{T_d}{H}\frac{1}{s}}{s^2\frac{I_b}{H}\frac{I_f}{H} + s\frac{I_b}{H}\frac{C}{H} + 1} \tag{18}$$

These reduce to the following steady-state equations (from eqs. (11) and (13)):

$$\omega_{b_{o_{1_{ss}}}} = \frac{T_d}{H}\frac{C}{H} + \frac{T_{U_G}}{H} + \frac{T_{U_G}}{H} \tag{19}$$

$$A_{f_{o_{1_{ss}}}} \approx -\frac{T_d}{H}t \tag{20}$$

For the closed loop, from equations (8) and (10),

$$\varphi_e = \frac{\omega_{LS}\frac{H}{K_{TG}}\left(s^2\frac{I_b}{H}\frac{I_f}{H} + s\frac{I_b}{H}\frac{C}{H} + 1\right) - \frac{T_d}{H}\frac{C}{H}\frac{H}{K_{TG}}\left(s\frac{I_f}{H}\frac{H}{C} + 1\right) - \frac{T_{U_G}}{H}\frac{H}{K_{TG}}}{s^3\frac{I_b}{H}\frac{I_f}{H}\frac{H}{K_{TG}} + s^2\frac{I_b}{H}\frac{C}{H}\frac{H}{K_{TG}} + s\frac{H}{K_{TG}} + 1} \tag{21}$$

$$A_f = \frac{\omega_{LS}\frac{I_b}{H} - \frac{T_d}{sH}\left(\frac{H}{K_{TG}}s + 1\right) + \frac{T_{U_G}}{H}s\frac{I_b}{H}\frac{H}{K_{TG}}}{s^3\frac{I_b}{H}\frac{I_f}{H}\frac{H}{K_{TG}} + s^2\frac{I_b}{H}\frac{C}{H}\frac{H}{K_{TG}} + s\frac{H}{K_{TG}} + 1} \tag{22}$$

And the steady-state equations (from eqs. (14) and (15)) become

$$\varphi_{e_{ss}} = \omega_{LS}\frac{H}{K_{TG}} - \frac{T_d}{H}\frac{C}{H}\frac{H}{K_{TG}} - \frac{T_{U_G}}{H}\frac{H}{K_{TG}} \tag{23}$$

$$A_{f_{ss}} \approx \omega_{LS}\frac{I_b}{H} - \frac{T_d}{H}t \tag{24}$$

It should be noted, as mentioned previously, that the term involving ω_{LS} in equation (24) is usually very small, and can be neglected in comparison with the external torque term.

Equation (23), which is plotted in figure 2. can be used to determine limits on K_{TG}/H and $(C/H)(H/K_{TG})$ by considering the values of allowable error and external disturbances expected. Since, in general, it is desirable to operate without excess forward-loop gain, this figure can be used to fix the value of K_{TG}/H, except that when C/H is selected, the product must be checked. The remaining normalized parameters are I_b/H, I_f/H, and C/H. The first of these is known as soon as the vehicle

is selected. As will be shown later, it is desirable for the quantity I_f/H to be small. Its actual size is determined by mechanical considerations of gyro design. For good system design, C/H should be selected on the basis of desired transient performance. This can be done more easily if the transfer function is simplified.

It would be desirable to reduce the form of equation (21) from a second-order numerator and third-order denominator to first and second orders, respectively. Considering first the denominator, it can be shown that if the s^3 term is very small compared to the s^2 term at $s = j\omega_n$, then, for reasonable values of damping ratio, the s^3 term may be dropped, with negligible effect on the system response. For equation (21) this requirement for simplification is stated mathematically as

A 4 4 3

$$\frac{I_b}{H}\frac{I_f}{H}\frac{H}{K_{TG}}\omega_n^3 << \omega_n^2\frac{I_b}{H}\frac{C}{H}\frac{H}{K_{TG}} \tag{25}$$

which reduces to

$$\frac{I_f}{H}\omega_n << \frac{C}{H} \tag{26}$$

or, alternatively, $I_f/C << 1/\omega_n$. Since I_f/C is the time constant of the gyro float response (sketch (c)), it is reasonable to expect that I_f/C will, in fact, be much less than $1/\omega_n$ if the float response time is not to degrade the over-all system response. This inequality must, of course, be checked when the design is completed.

The numerator of equation (21) should now be considered. Since the denominator will attenuate greatly all frequencies higher than ω_n, it seems reasonable to compare the relative sizes of the numerator terms at ω_n. If this is done, the numerator term associated with ω_{LS}, at $s = j\omega_n$, becomes

$$\omega_n^2\frac{I_b}{H}\frac{I_f}{H} + \omega_n\frac{I_b}{H}\frac{C}{H} + 1$$

When equation (26) is applied, it can be seen that the first term is negligible compared to the second and can be dropped. Further simplification of the numerator can be made by comparing the numerator term associated with T_d at $s = j\omega_n$,

$$\omega_n\frac{I_f}{H}\frac{H}{C} + 1$$

With equation (26) written as

$$\frac{I_f}{H}\frac{H}{C}\omega_n << 1$$

it can be seen that the term associated with T_d reduces to unity. Thus with the one assumption of equation (26), equation (21) becomes

$$\varphi_e = \frac{\omega_{LS}\frac{H}{K_{TG}}\left(\frac{I_b}{H}\frac{C}{H}s + 1\right) - \frac{T_d}{H}\frac{C}{H}\frac{H}{K_{TG}} - \frac{T_{UG}}{H}\frac{H}{K_{TG}}}{s^2\frac{I_b}{H}\frac{C}{H}\frac{H}{K_{TG}} + s\frac{H}{K_{TG}} + 1} \qquad (27)$$

A4443

This equation is independent of the float inertia, I_f, and, as would be expected from the remarks concerning the inequality of equation (26), equation (27) could be obtained directly from sketch (c) by setting $I_f = 0$.

Rather common symbols for second-order equations may be used to write equation (27) as

$$\varphi_e = \frac{\omega_{LS}\frac{H}{K_{TG}}(\tau s + 1) - \frac{T_d}{H}\frac{C}{H}\frac{H}{K_{TG}} - \frac{T_{UG}}{H}\frac{H}{K_{TG}}}{\frac{s^2}{\omega_n^2} + \frac{2\zeta}{\omega_n}s + 1} \qquad (28)$$

where

$$\tau = \frac{I_b}{H}\frac{C}{H} \qquad (29)$$

$$\omega_n = \sqrt{\frac{H}{I_b}\frac{H}{C}\frac{K_{TG}}{H}} \qquad (30)$$

$$\zeta = \frac{1}{2}\sqrt{\frac{H}{K_{TG}}\frac{H}{C}\frac{H}{I_b}} \qquad (31)$$

It should be noted that these three quantities are related by

$$2\zeta\omega_n\tau = 1 \qquad (32)$$

and further, subject to the restrictions of equation (26), they are independent of I_f/H.

From dimensionless transient response curves, such as those given by Truxal on pages 38 to 41 (ref. 4), one can see that if

$$\tau\omega_n < 1 \tag{33}$$

the over-all transient response will have only slightly more overshoot than a simple second-order system with no zero. Thus the system can be designed for a damping ratio, ζ, in the region of 0.5 to 1.0 (resulting in $\tau\omega_n \leq 1$, from equation (32)) with assurance of reasonable transient response.

Selecting a damping ratio of 0.7 (giving $\tau\omega_n = 0.7$) and solving equation (31) for C/H gives:

$$\frac{C}{H} = \frac{1}{2}\frac{H}{K_{TG}}\frac{H}{I_b} \tag{34}$$

Changing the desired damping ratio will of course change the numerical coefficient in equation (34).

The system design has now been completed, presumably satisfactorily. It is desirable to be able to check the behavior of this system when the target star is occulted, which is theoretically the same as setting $K_{TG} = 0$. When the inequality of equation (26) is applied to equation (17), the following equation is obtained:

$$\omega_{b_{o1}} = \frac{\frac{T_d}{H}\frac{C}{H} + \frac{T_{U_G}}{H} + \frac{T_{TG}}{H}}{s\frac{I_b}{H}\frac{C}{H} + 1} \tag{35}$$

This is now effectively a first-order system with a time constant

$$\tau_{o1} = \frac{I_b}{H}\frac{C}{H} = \tau \tag{36}$$

The complete design procedure developed may be summarized as follows: (1) select a value for H, using equation (16); (2) select a value for K_{TG}/H from figure 2(a); (3) compute the value of C/H required for 0.7 damping from equation (34) (or for any other damping ratio from equation (31)); (4) check figure 2(b) to see that the resultant $(C/H)(H/K_{TG})$ is satisfactory; (5) compute values for τ and ω_n from equations (29) and (30); (6) check to see that the inequality of equation (26) is

satisfied; (7) check to see that the numerator zero does not deteriorate the performance, using equation (33); and (8) examine the open-loop performance, using equation (35).

ERROR AND TORQUE GENERATOR LIMITING

In actual practice, the signal from the sensor will be a voltage that will be limited at some relatively small angle, compared to the maximum error angle the sensor can detect. Also, there will be some maximum torque, T_{TG}, available from the torque generator. However, since the sensor and torque generator are adjacent, they may be combined as shown in sketch (c). During the time the system is limited, it is operating open-loop, and equations (17) through (20) apply. Equation (19) shows that if the torque-generator torque (or the error) is limited at some maximum value, the vehicle will have a corresponding maximum angular velocity. If very large initial errors exist, the gyros will accelerate the vehicle to this maximum angular velocity. The vehicle will then coast at this velocity until the error becomes less than the limiting value. Since the vehicle is thus essentially passive during this coast period, the size of the initial error will not affect the final portion of the transient after a linear error signal becomes available. Thus, system stability is essentially independent of the size of the initial error, although the total settling time will be lengthened as the initial error is increased.

An estimate of the time, t_{lim}, during which the error is limited, can be made by means of steady-state characteristics. If the vehicle is assumed to rotate at its maximum angular velocity, $\omega_{b_{max}}$, until the error becomes equal to the limited value, $\varphi_{e_{lim}}$, then it can be stated mathematically that

$$t_{lim} = \frac{\varphi_{e_o} - \varphi_{e_{lim}}}{\omega_{b_{max}}} \tag{37}$$

This equation assumes that the time to accelerate to $\omega_{b_{max}}$ is negligible. Equation (19) can be written for this purpose as

$$\omega_{b_{max}} \cong \frac{T_{TG}}{H} = \frac{\varphi_{e_{lim}} K_{TG}}{H}$$

Thus

$$t_{lim} = \frac{\varphi_{e_o} - \varphi_{e_{lim}}}{\varphi_{e_{lim}}} \frac{H}{K_{TG}} \tag{38}$$

For a second-order system, such as the one represented by equation (27), it can be shown that if the damping ratio is about 0.7, the settling time from an initial step in error to 2 percent of the initial value is comparable to the natural period. If the velocity of the vehicle when the error becomes unlimited is neglected and the final error is assumed to be about 2 percent of the limiting error, then the linear portion of the settling time can be approximated by τ_n. Thus the total settling time may be approximated by

$$t_{set} = t_{lim} + \tau_n \tag{39}$$

In this equation τ_n is too large, since the vehicle velocity at the limiting error is assumed to be zero, and t_{lim} is too small, since the initial acceleration is assumed to occur instantaneously.

SAMPLE DESIGNS

A set of equations and curves has now been developed which will enable a control system to be designed with satisfactory transient response and steady-state errors. These curves and equations will now be used to design a sample system for the OAO. The requirements for this satellite are as follows:

$$\left|\varphi_{e_{ss}}\right| \leq 0.1 \text{ second of arc}$$

$$t_c \approx 105 \text{ min}$$

The satellite moment of inertia is assumed to be

$$I_b = 10^{10} \text{dyne cm sec}^2$$

and the maximum values of disturbances are assumed as

$$\left|\omega_{LS}\right| = 2.4\times10^{-8} \text{radian/sec} \approx 0.005^{\circ}/\text{hr}$$

$$\left|T_d\right| = 100 \text{ dyne cm}$$

The necessary gyro constants will be assumed as

$$\left|T_{UG}\right| = 1 \text{ dyne cm}$$

$$\frac{I_f}{H} = 1.4\times10^{-3} \text{sec}$$

To minimize cross coupling, the gyro float angle is limited at 3°. From equation (16) it is found that $H = 1.2\times10^{7}$ dyne cm sec. Allowing an additional margin of safety and using a round number gives

$$H = 2\times10^{7} \text{ dyne cm sec}$$

Then

$$\left|\frac{T_{U_G}}{H}\right| = 5\times10^{-8} \text{ sec}^{-1}$$

$$\left|\frac{T_d}{H}\right| = 5\times10^{-6} \text{ sec}^{-1}$$

$$\frac{I_b}{H} = 5\times10^{2} \text{ sec}$$

To meet the steady-state error requirement ($|\varphi_{e_{ss}}| < 0.1$ second of arc), the following gain and damping requirements are determined from figure 2:

due to $|\omega_{LS}|$

$$\frac{K_{TG}}{H} \geq 0.05 \text{ sec}^{-1}$$

due to $\left|\frac{T_{U_G}}{H}\right|$

$$\frac{K_{TG}}{H} \geq 0.1 \text{ sec}^{-1}$$

due to $\left|\frac{T_d}{H}\right|$

$$\frac{K_{TG}}{H}\frac{H}{C} \geq 10 \text{ sec}^{-1}$$

For $K_{TG}/H = 0.1 \text{ sec}^{-1}$, which is the minimum allowable value, $I_b/H = 5\times10^{2}$ sec, and $\zeta = 0.7$, it is found from equation (34) that $C/H = 0.01$. Checking for the $(K_{TG}/H)(H/C)$ product gives

$$\frac{K_{TG}}{H}\frac{H}{C} = \frac{0.1}{0.01} = 10$$

which is satisfactory. Values for τ and ω_n can now be found by using equations (29) and (30), which give $\tau = 5$ sec and $\omega_n = 0.14$ radian/sec. The inequality of equation (26) becomes $2\times10^{-4} << 10^{-2}$, which is satisfied.

The value of the numerator zero is found to be (from eq. (32)) $\tau\omega_n = 0.7$. Since this is less than 1, the zero will have little effect on the over-all response (as previously discussed for eq. (33)). The time constant of the open-loop response is found from equation (36) as

$$\tau_{o1} = 5 \text{ sec}$$

Thus, the over-all design appears satisfactory, and the table below lists the values of the parameters and response characteristics of the system.

A
4
4
3

$I_b = 10^{10}$ dyne cm sec^2	$\zeta = 0.7$
$H = 2\times10^{7}$ dyne cm sec	$\omega_n = 0.14$ radian/sec
$\frac{I_f}{H} = 1.4\times10^{-3}$ sec	$\tau_n = 45$ sec
$\frac{K_{TG}}{H} = 0.1$ sec^{-1}	$\tau_{o1} = 5$ sec
$\frac{C}{H} = 0.01$	

Equations (38) and (39) can be used to estimate the settling time of this system. With an initial error of 60 seconds of arc and an assumed limit level of 5 seconds of arc,

$$t_{set} = 155 \text{ seconds}$$

This value is not unreasonable, and it can be reduced, if desired, by raising the limit level.

ANALOG SIMULATION

To check on the analytical work just presented, an analog study was made of the gyro control system. The three-dimensional problem was simulated; that is, three gyros and three single-axis sensors were mounted on the satellite.

The gyros were mounted, as shown in sketch (d), so that the sensitive axis of the x gyro was alined along the satellite x axis,

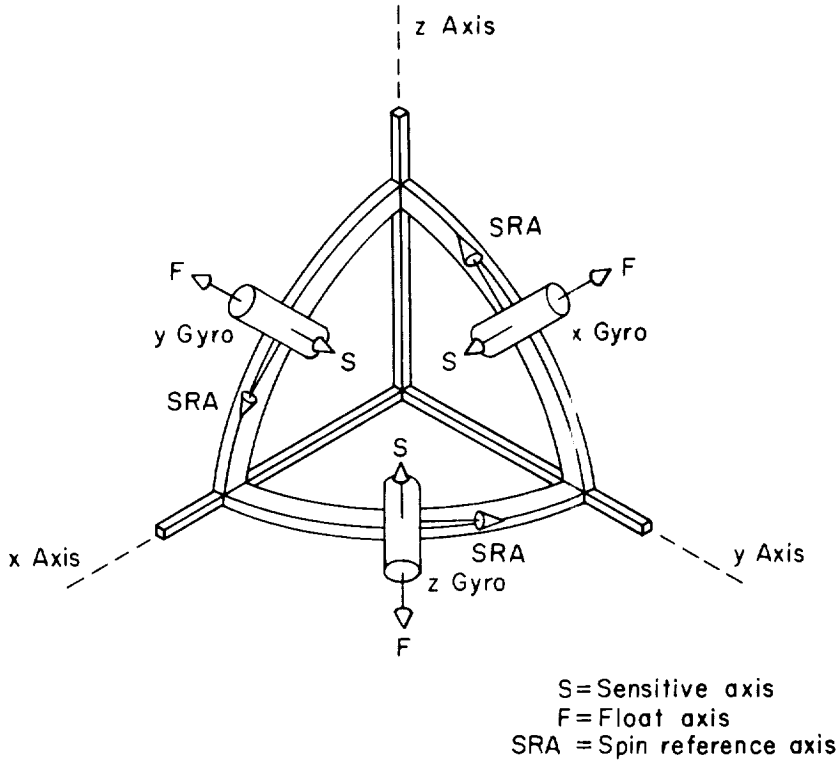

Sketch (d)

and the float axis was alined at 45° to the satellite y axis. The sensitive axis of the y gyro was along the satellite y axis, and its float axis was 45° from the satellite z axis. The z gyro was alined in a corresponding fashion. The advantage of this gyro mounting arrangement (suggested by the Reeves Instrument Corporation) is that the sum of the three H vectors is equal to zero. As a result, changes in wheel drive frequency will not exert a torque on the satellite.

Figure 3 shows the analog diagram for the system. Figure 3(a) shows one channel of the control system; the other two are identical. Figures 3(b) and 3(c) show the necessary torque and angular velocity resolutions, resulting from the 45° angle between float and satellite axis, and from the rotation of the float, A_f, about the float axis. The broken lines in figure 3(a) complete the signal paths when only a single-axis system is being considered.

Figure 4 shows the response of the system to a step position input about one of the axes. It was assumed that all three float angles were initially zero and that the error limit was 5 seconds of arc.[1] The responses for step inputs about the other two axes had the same characteristics, with no indication of cross coupling. Runs made with initial errors about two or three axes also showed the same response characteristics, with no cross coupling.

Figure 5 shows the response to the same input, but this time with an initial, very large float angle of the x gyro, A_{fx}, of 15°. The input was only in the x axis and, as shown in figure 5, the response of this channel was essentially the same as in figure 4. The cross coupling produced error and float angular velocity in both the y and z channels. The responses of these two channels were very similar, although only the y channel is shown. Additional runs were made in which the other gyros had initial conditions, and the responses were very similar to those shown in figure 5.

The effect of torque input was also studied on the analog computer, with the results shown in figure 6. Here there was a step input of torque of 100 dyne cm, and, as expected, the error angle reached a steady-state value of 0.1 second of arc, and the float angle increased at a constant rate. The other channels showed no signs of cross coupling.

Since the cross coupling is small, a study of the effect of varying the parameters can be carried out on a single-axis system and the predicted response characteristics from the linear analysis should be reasonably valid. A simplified data analysis of figure 4 indicates a system damping ratio, in the linear region, of about 0.7 and a natural period of 45 seconds. The settling time, computed from equations (38) and (39) using φ_{e_o} = 11 seconds of arc and $\varphi_{e_{lim}}$ = 5 seconds of arc, is 57 seconds. Thus, the values from the analog simulation agree very well with the predicted values.

EXPERIMENTAL EVALUATION

Some experimental work was carried out on a low-friction, three-degree-of-freedom platform. The platform, shown in figure 7 and described in more detail in reference 1, was supported on an air bearing to obtain extremely low friction levels. This platform had a considerably smaller moment of inertia than the OAO, and the gyros used on the platform were specially modified single-degree-of-freedom gyros. The particular constants are

[1]With the value of torque generator gain used, this corresponds to a maximum torque-generator torque of 50 dyne cm.

$$I_b = 2.4\times10^{8}\text{dyne cm sec}^2$$

$$H = 9.6\times10^{6}\text{dyne cm sec}$$

$$I_f = 1.4\times10^{4}\text{dyne cm sec}^2$$

$$C = 2.7\times10^{5}\text{dyne cm sec}$$

Computing the same normalized design ratios used previously gives

$$\frac{I_b}{H} = 25 \text{ sec}$$

$$\frac{I_f}{H} = 1.5\times10^{-3}\text{sec}$$

$$\frac{C}{H} = 0.028$$

Experimentally, a gain of $K_{TG}/H = 1.7 \text{ sec}^{-1}$ was used to obtain reasonable response. From equation (23) it can be shown that the following inputs can be tolerated for $|\varphi_{ess}| \leq 0.1$ second of arc:

$$|\omega_{LS}| \leq 8.4\times10^{-7}\text{radian/sec}$$

$$|T_{UG}| \leq 8 \text{ dyne cm}$$

$$|T_d| \leq 290 \text{ dyne cm}$$

As will be shown later, it was found that the platform had random errors of about 1.0 second of arc. From equation (23), it is found that a torque of about 3000 dyne cm would produce a steady-state error of this value.

The parameters indicated for the system may be used to compute the response characteristics. For damping ratio, equation (31) is used to obtain

$$\zeta = 0.46$$

For natural frequency, equation (30) is used to obtain

$$\omega_n = 1.6 \text{ radians/sec}$$

which corresponds to a natural period of

$$\tau_n = 3.9 \text{ sec}$$

These values indicate that the response is reasonably damped, but faster than necessary. The speed of response cannot be reduced (by reducing the gain) however, without causing an increased steady-state error. The inequality of equation (26) is satisfied since

$$2.4\times10^{-3} << 2.8\times10^{-2}$$

The value of τ is calculated from equation (29), giving

$$\tau = 0.7 \text{ sec}$$

and the value of $\tau\omega_n$ is found to be

$$\tau\omega_n = 1.1$$

This value does not satisfy the inequality of equation (33), so the numerator term of equation (28) cannot be completely neglected in estimating the response; however, its effect is only to increase the initial overshoot by about 15 percent. The time constant, for the open-loop system, from equation (36), is

$$\tau_{o1} = \tau = 0.7 \text{ sec}$$

The following table lists the parameters and the system response characteristics:

$I_b = 2.4\times10^8$ dyne cm sec^2	$\zeta = 0.46$
$H = 9.6\times10^6$ dyne cm sec	$\omega_n = 1.6$ radians/sec
$I_f/H = 1.5\times10^{-3}$ sec	$\tau_n = 3.9$ sec
$C/H = 0.028$	$\tau_{o1} = 0.7$ sec
$K_{TG}/H = 1.7$ sec^{-1}	

Figure 8(a) shows the experimental transient response of the platform to an initial error. No limiting occurs in the sensor or torque generator, and the natural frequency and damping compare favorably with the computed values. It can be seen that accuracy of control is only about 1 second of arc. It was felt that this large error was caused by external disturbances acting on the platform. Figure 8(b) shows the analog simulation which used the parameters of the experimental platform and included "random" steps of external torque having a magnitude of about 1000 dyne cm. It can be seen that the general character of the initial response is essentially the same. The amplitude of response of the experimental

platform to external disturbances is about three times as large as that of the analog system to the analog disturbance. Since the analog disturbance was 1000 dyne cm, this would indicate an experimental disturbance of about 3000 dyne cm, which agrees very well with the value of disturbance torque previously estimated. The system responses about the other axes were similar and no cross coupling between the channels was noted.

CONCLUDING REMARKS

The results of this investigation have shown that single-degree-of-freedom integrating gyros, acting as torque sources, can provide precise attitude control of a satellite. The transient behavior of such a system is reasonably rapid and well damped. The steady-state errors of the system, in response to external disturbances and motion of the line of sight, appear to be sufficiently small for many applications. The gyros act as rate sensors as well as torque sources, so that no rate stabilization networks are required, and when no error sensor is available, the vehicle is still rate stabilized. Hence, a major advantage of a gyro control system is that when the target is occulted, an alternate reference is not required. In addition, because of the torque multiplying effect of the gyro, the torque generator and, therefore, the driving amplifier, can be smaller than would be the case for inertia wheels, where the torque is developed directly by the motor.

A 4 4 3

Compared to an inertia wheel system, one disadvantage of the gyro system is that only about 5 percent (for a float angle of $\pm 3^{\circ}$) of the gyro momentum is available for active control; thus a larger or faster turning wheel is required. Other disadvantages, which are not mentioned in this report, are the additional moving parts and weight required for the gyro float and case, which may have to be temperature controlled, requiring additional power. These advantages and disadvantages, along with total system weight and power, must be considered when a system for an actual satellite is being designed.

Ames Research Center
National Aeronautics and Space Administration
Moffett Field, Calif., July 12, 1961

REFERENCES

1. White, John S., and Hansen, Q. Marion: Study of Systems Using Inertia Wheels for Precise Attitude Control of a Satellite. NASA TN D-691, 1961.

2. White, John S., Shigemoto, Fred S., and Bourquin, Kent: Satellite Attitude Control Utilizing the Earth's Magnetic Field. NASA TN D-1068, 1961.

3. Triplett, William C.: Design Considerations for an Orbiting Astronomical Observatory. ARS Paper, 1184-60, 1960.

4. Truxal, John G.: Control System Synthesis. McGraw-Hill Book Co., Inc., 1955.

A
4
4
3

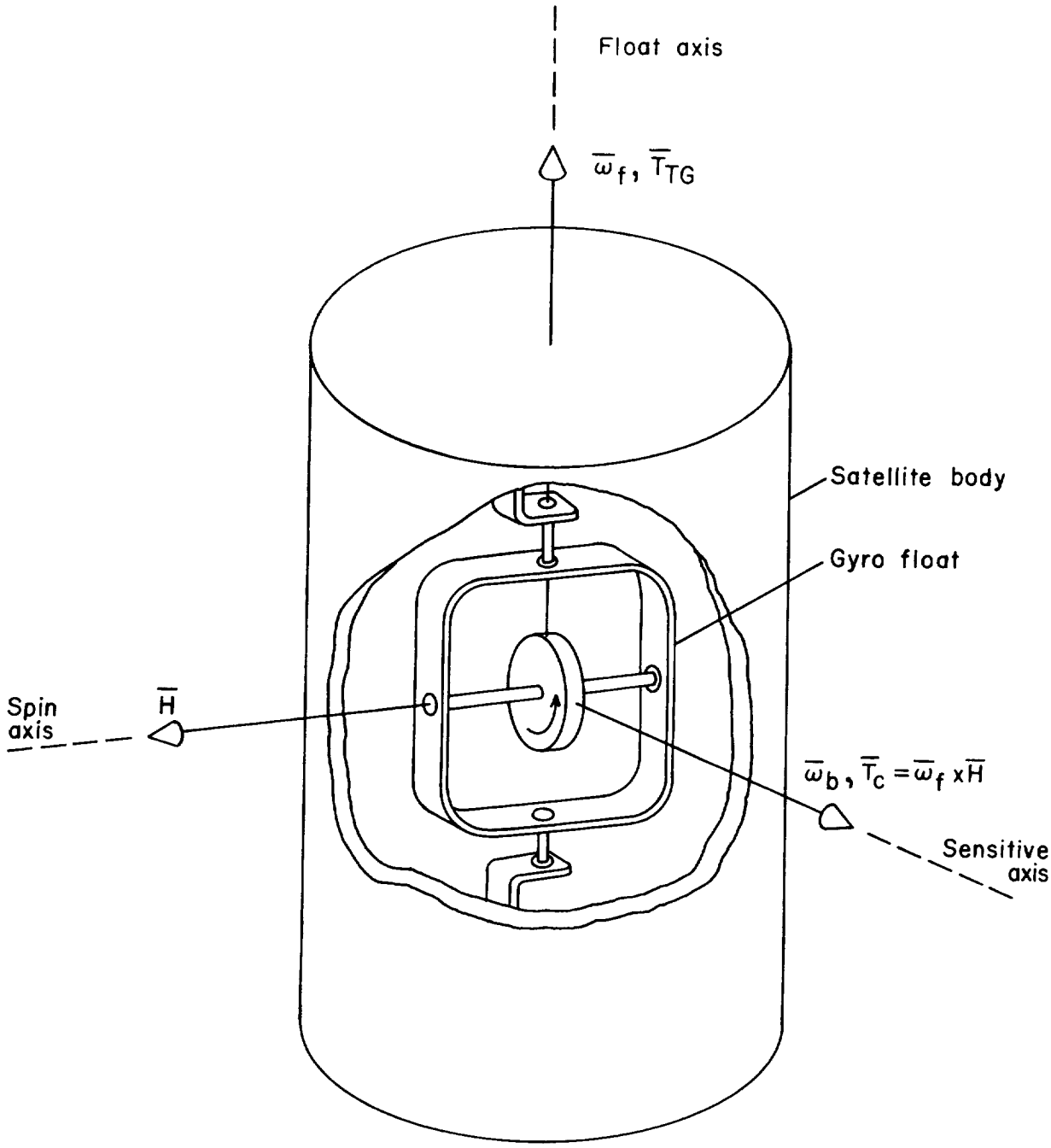

Figure 1.- Pictorial view of a single-degree-of-freedom gyro used in satellite.

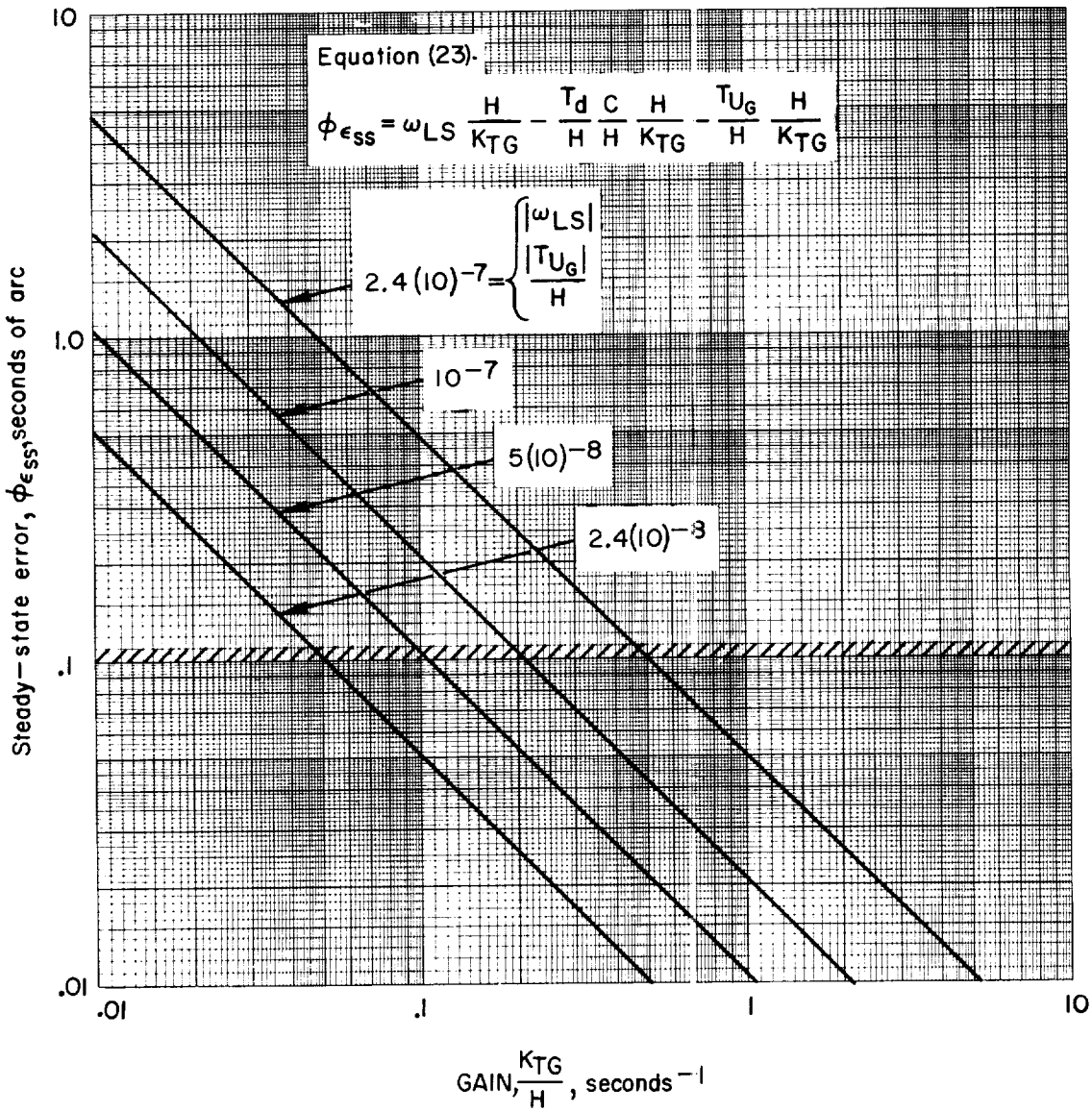

(a) ω_{LS} and T_{U_G} as disturbances.

Figure 2.- Gain requirements vs. steady-state error.

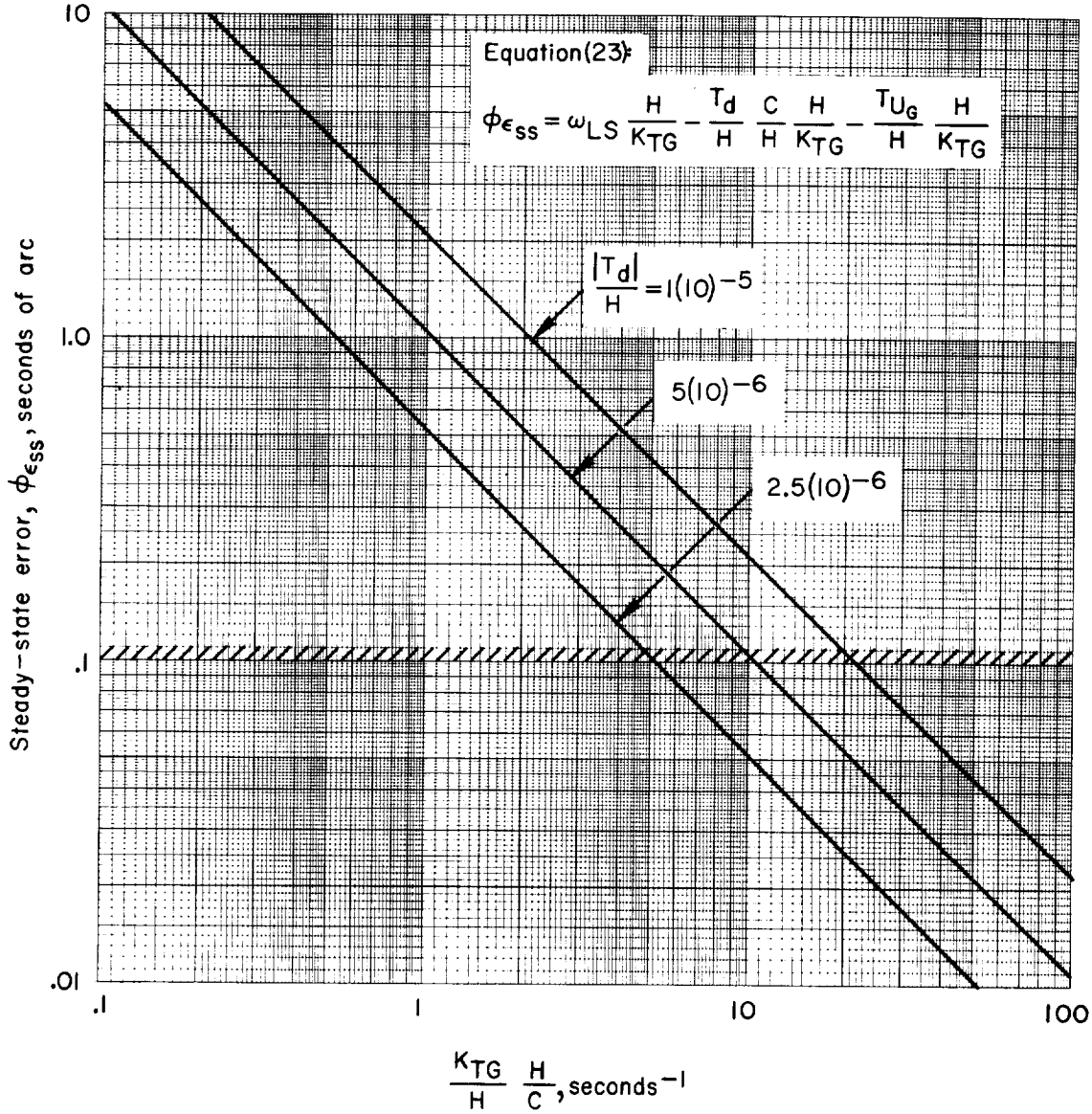

(b) T_d as disturbance.

Figure 2.- Concluded.

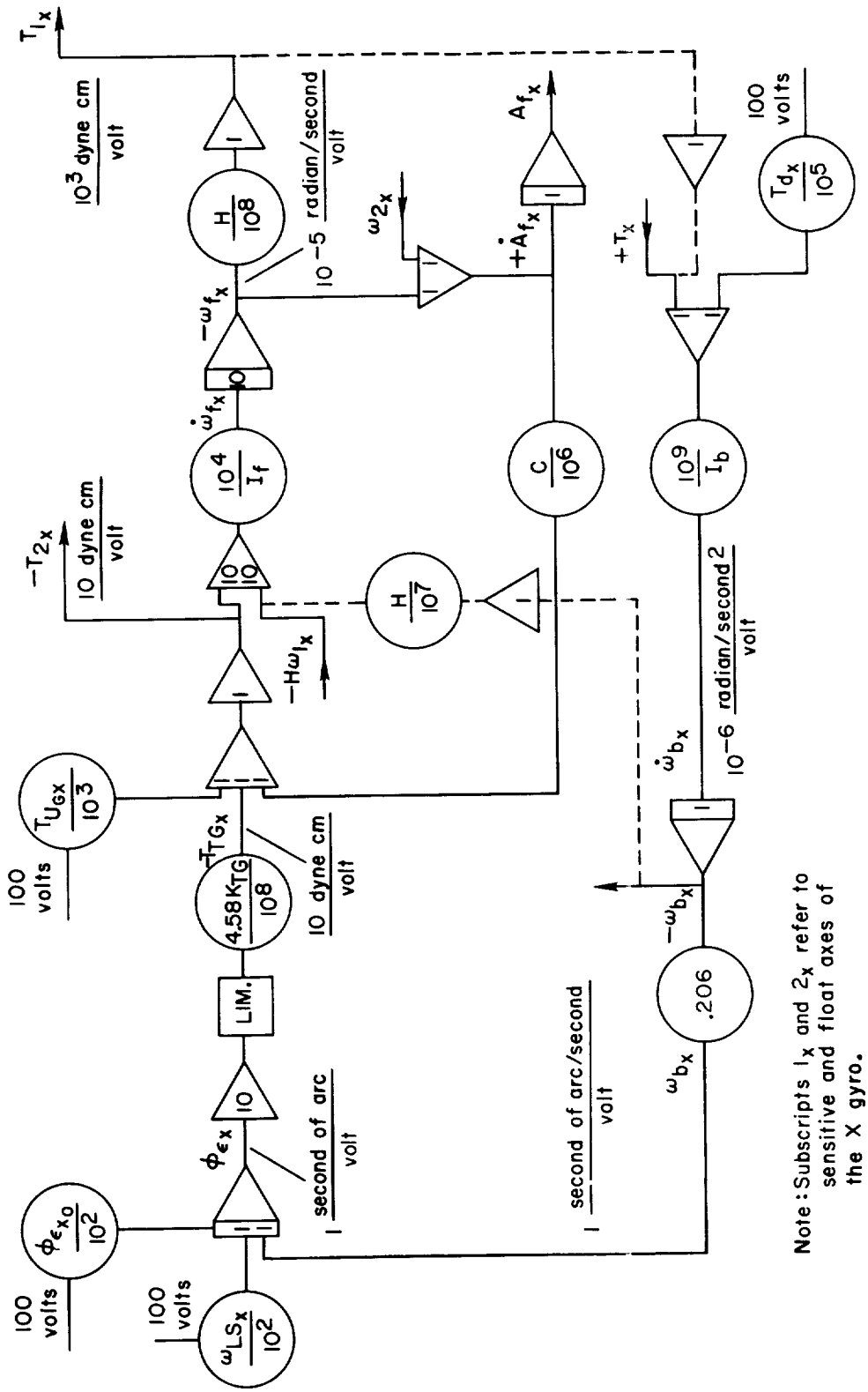

(a) Control loop of one channel.

Figure 3.- Analog diagram of three-axis control system.

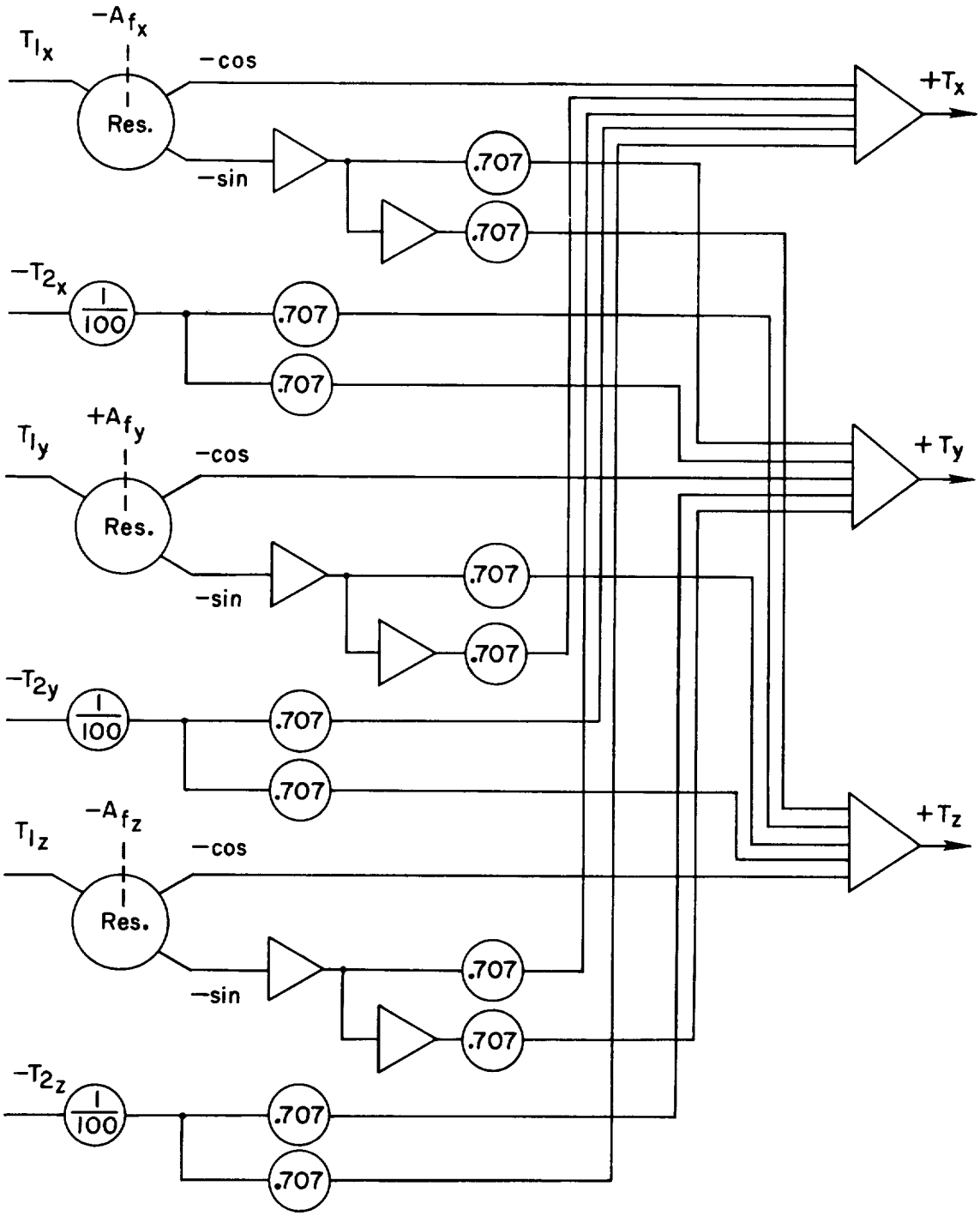

(b) Torque resolution.

Figure 3.- Continued.

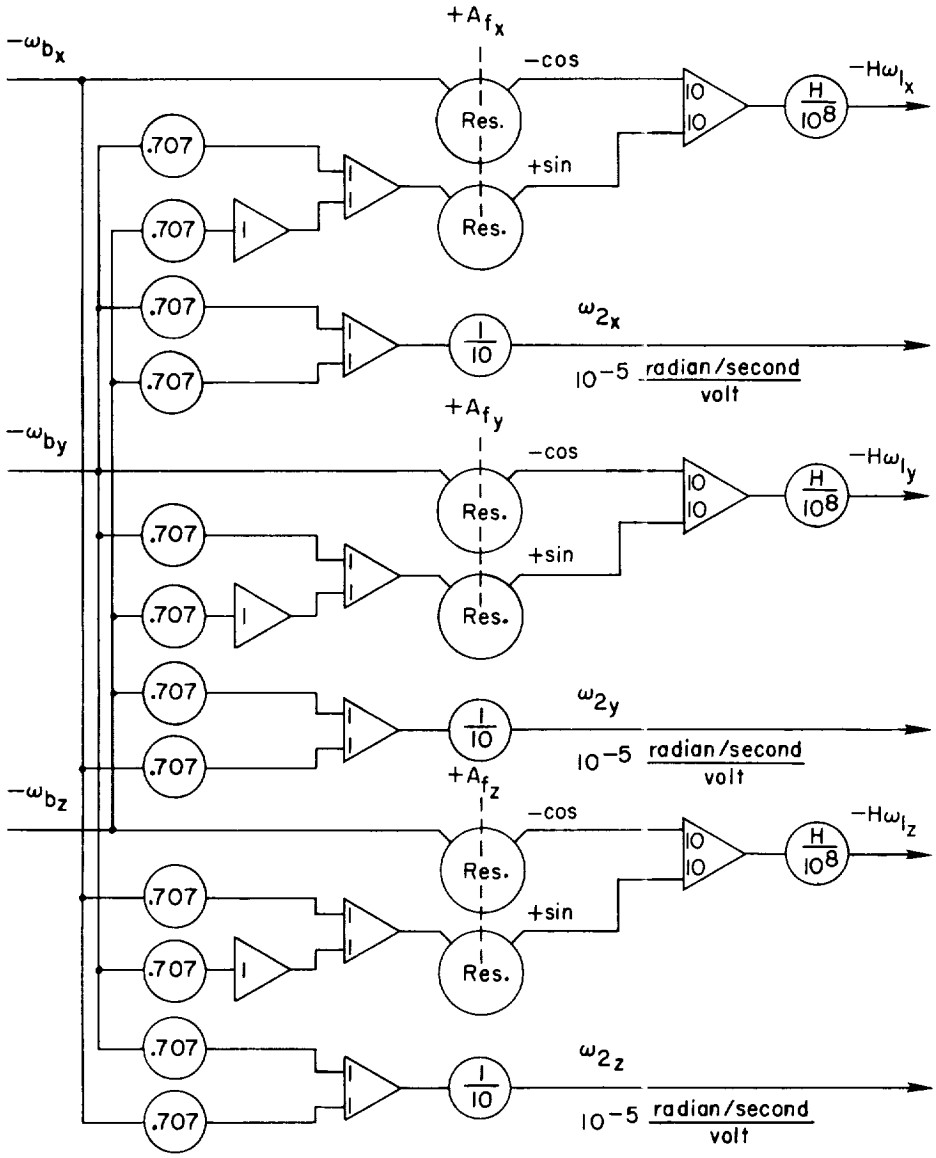

(c) Angular velocity resolution.

Figure 3.- Concluded.

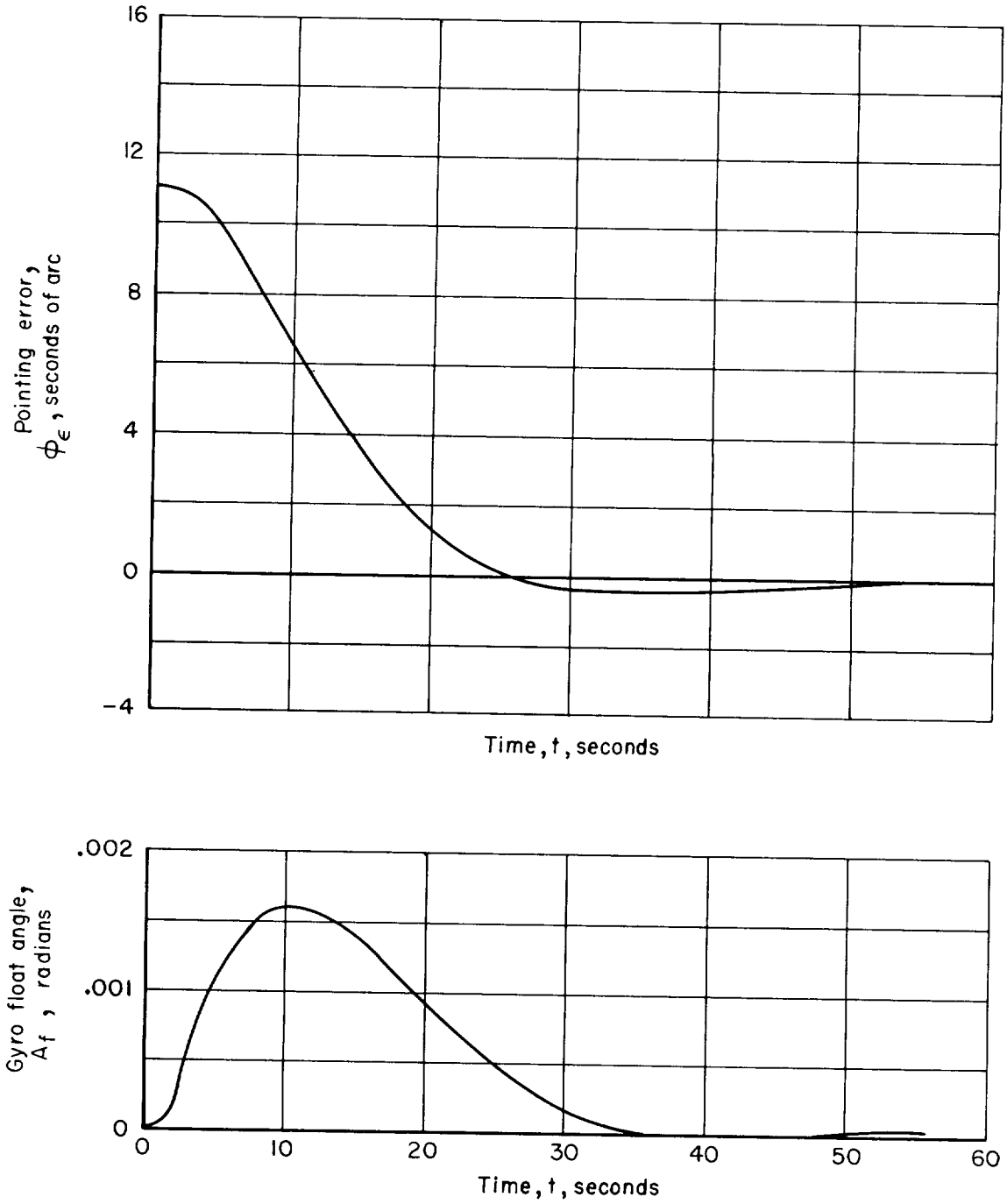

Figure 4.- Analog system transient response with all initial float angles zero.

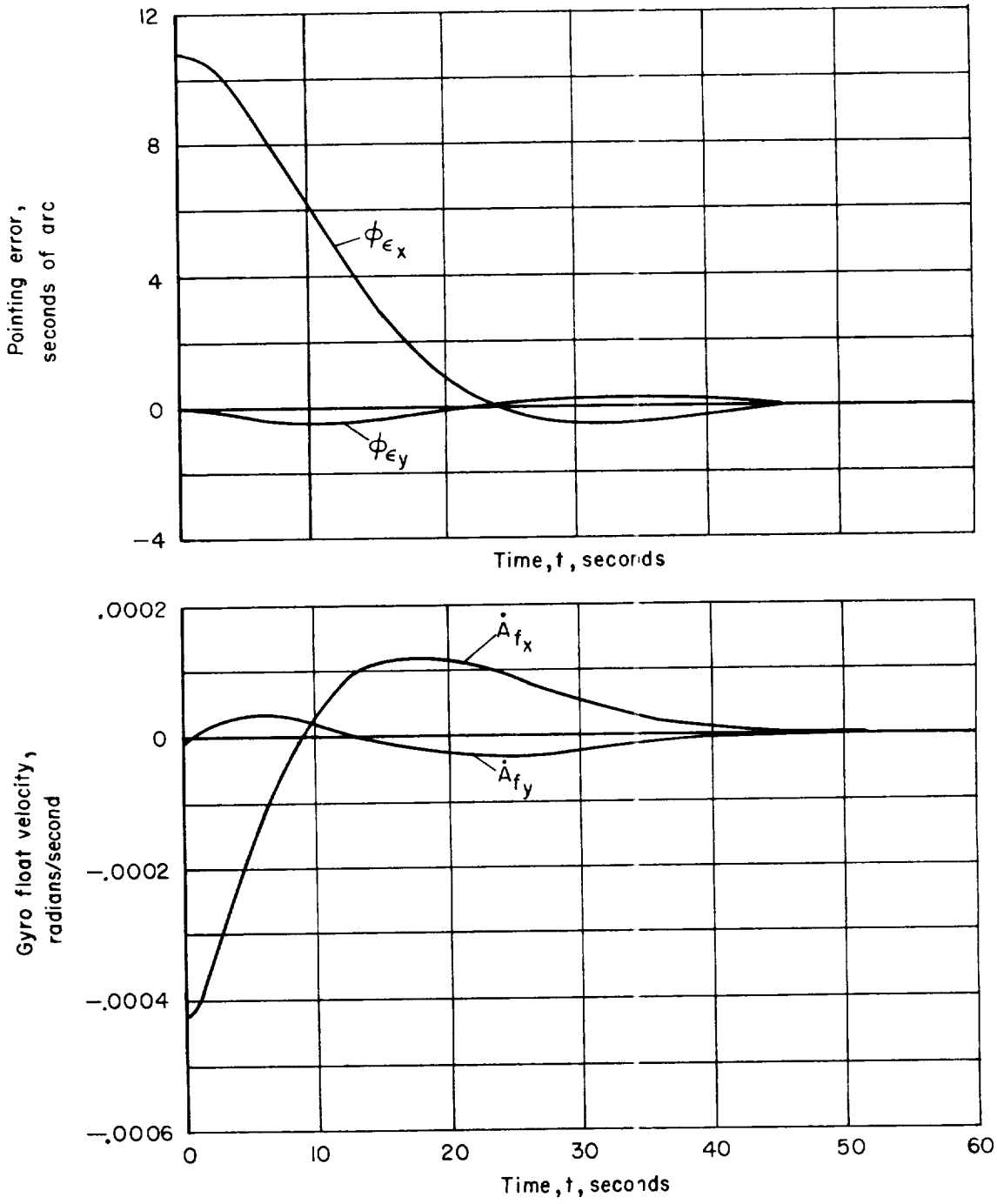

Figure 5.- Analog system transient response with 15° initial float angle on x gyro.

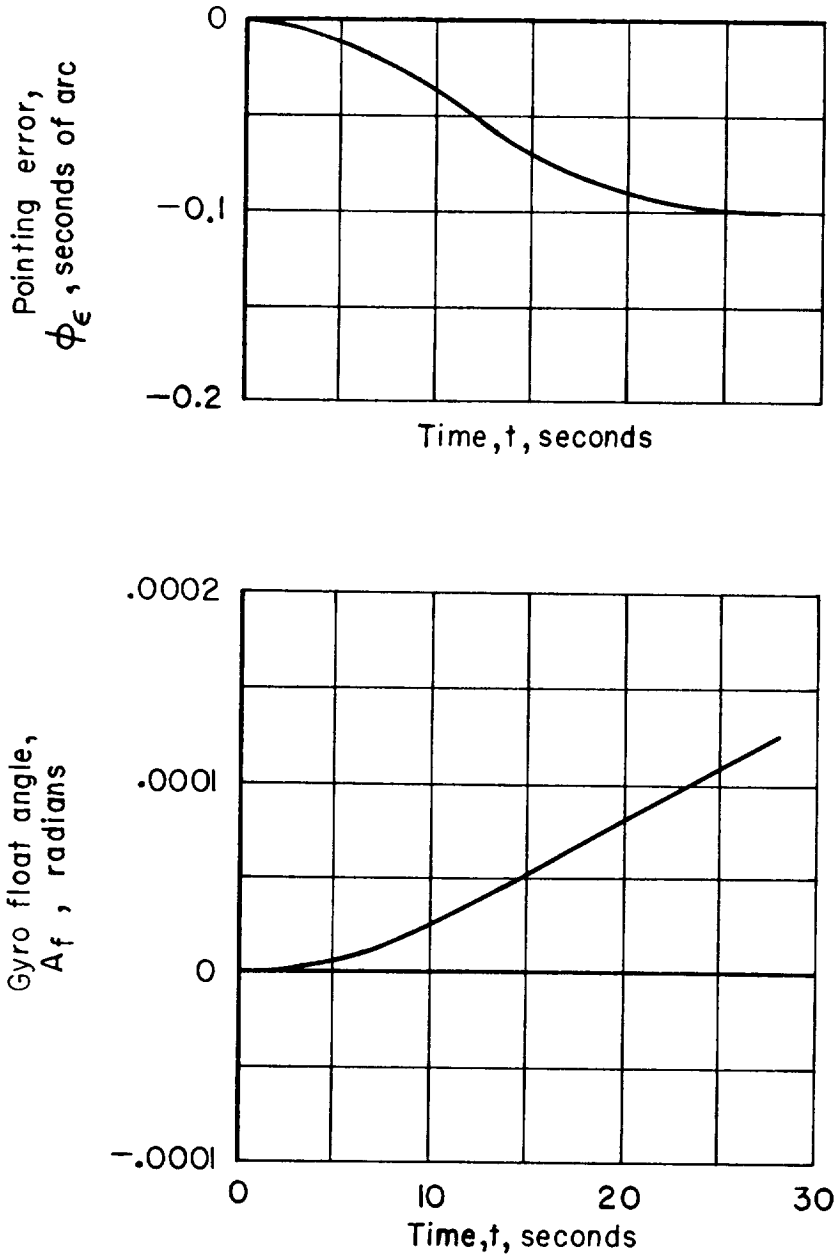

Figure 6.- Analog system transient response to step input of 100 dyne cm disturbance torque.

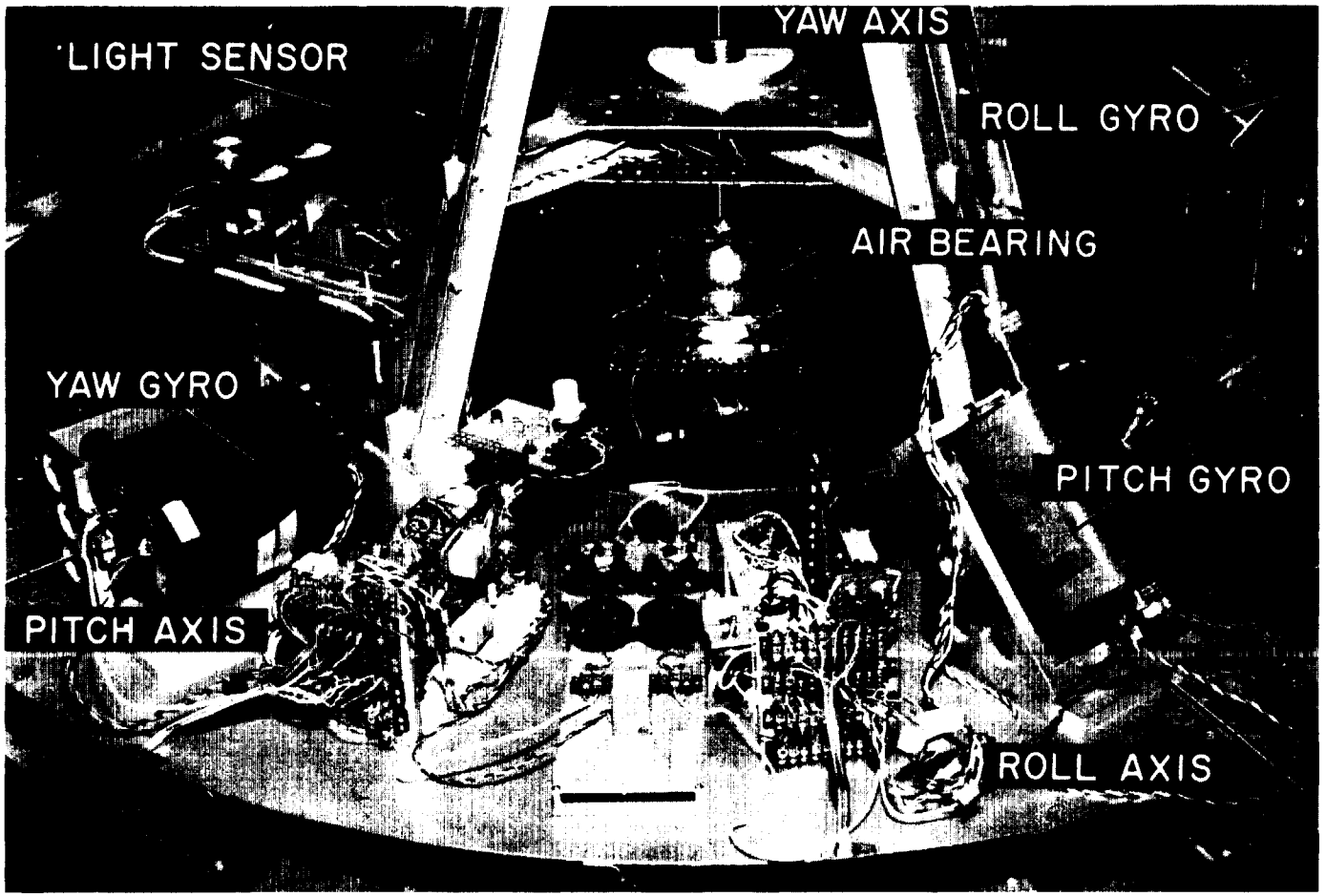

A-27204.1

Figure 7.- Satellite attitude control test platform with gyros.

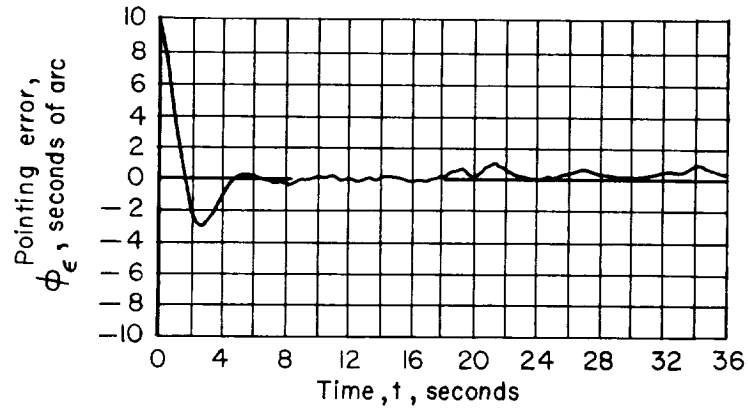

(a) Experimental system response.

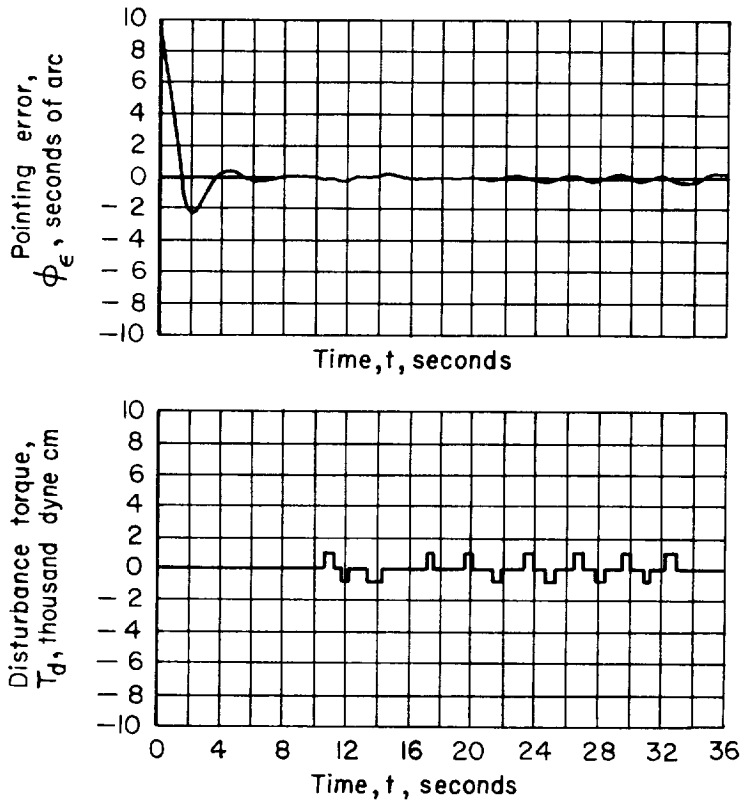

(b) Analog system response.

Figure 8.- Response of platform to an initial step position input accompanied by disturbance torques.